

Chapter 1

Introduction

There has been a rapid and ceaseless increase in communication traffic in global networks for the distribution of digital content, such as video streams, visual content, and big data. A forecast of the growth of communication traffic reports an increase in the global internet protocol (IP) traffic, as plotted in Fig. 1.1: the traffic increases beyond 100 exabyte (EB) per month and beyond 1 zettabyte (ZB) per annum in 2017.¹ Fixed internet traffic occupies the major portion in the meantime; mobile data traffic grows more rapidly and will reach the fixed internet traffic some years after 2020. Such a burst of IP traffic creates demand for greater transmission capacity in optical networks spreading over personal mobile terminals, fiber-to-the-home (FTTH) networks, local-area networks (LANs), datacenters, metro networks, and backbone core networks. Therefore, high-capacity optical networks at 100 gigabytes per second (Gb/s) and beyond are essential for the infrastructure that supports the modern information and intelligence era.

High-speed photonic devices are used in optical communication equipment for high-capacity data transmission in optical networks. Among high-speed photonic devices, optical modulators accommodated in optical transceivers (in which optical transmitters and optical receivers are co-packaged) play crucial roles in high-capacity optical networks because optical modulators permit high-quality optical signal generation in high-transmission capacity. The production of optical modulators with conventional design and fabrication platforms requires the assembly of dielectric crystals for phase shifters, RF electrodes for high-speed electrical signals, and elements for optical beam coupling such as mirrors and focusing/collimating lenses.²⁻⁵ With such conventional production approaches, compact-form-factor optical transceivers—which are now essential to enhance the transmission capacity of modern optical networks—have not been realized because conventional optical modulators have a considerable footprint in optical transceivers.

Photonic integration technology has disrupted design and fabrication platforms with on-chip integration, and thus phase-shifter waveguides, planar RF transmission electrodes, and other photonic components have been

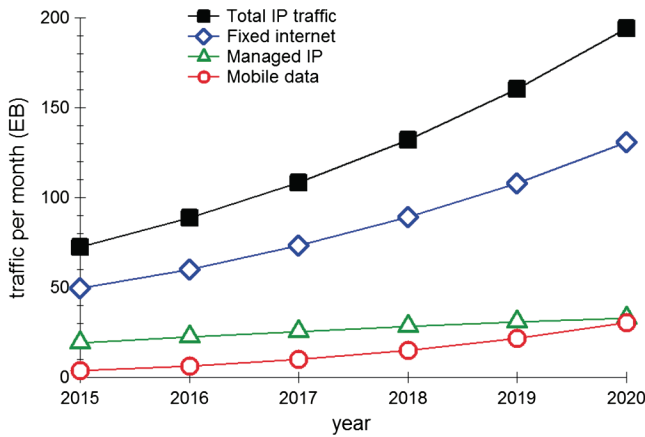


Figure 1.1 Communication traffic per month plotted vs year.¹

integrated monolithically on small-footprint photonic chips.^{6,7} The groundbreaking integration technology has enabled the design and fabrication platforms of compound-semiconductor photonics, silicon photonics, and polymer photonics, and has opened the way to compact-form-factor optical transceivers. Photonic integration platforms now support the technology roadmaps for compact transceivers with high-transmission capacity. A trend in footprint reduction for CFP-series optical transceivers (a series of compact-form-factor pluggable optical transceivers), is illustrated in Fig. 1.2. The footprint, defined as a product of width W and length L , is plotted against

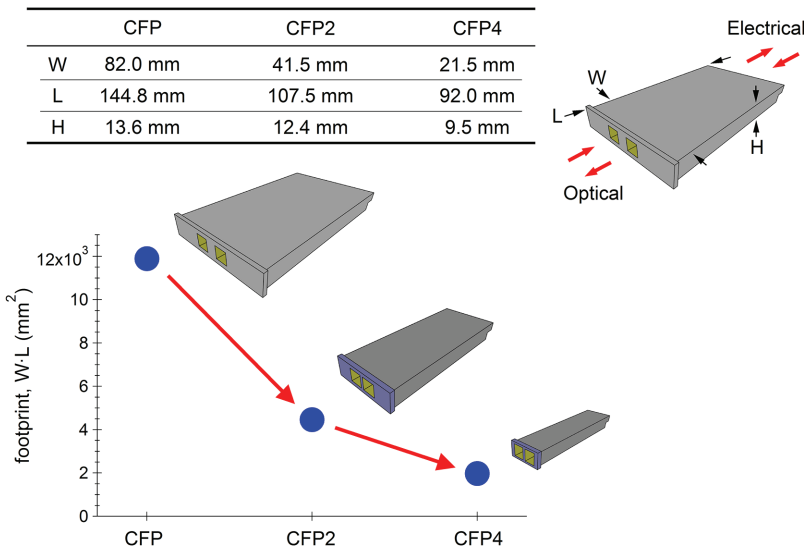


Figure 1.2 Footprint reduction for CFP-series compact-form-factor, pluggable optical transceivers.

CFP-series generation using physical-dimension data in CFP multi-source agreement (CFP-MSA) as an example of compact optical transceivers⁸ [the term CFP stands for “C form-factor pluggable,” where C is the number 100, or *centum* in Latin]. An almost-one-order reduction in footprint is observed in the refinements from CFP to CFP4. In compact-form-factor, pluggable optical transceivers such as the CFP series, the optical input/output (I/O) ports for optical data are aligned on the front panel of the transceiver housing, whereas the electrical input/output ports for electrical data are on the back edge of the transceiver housing, as indicated in the inset of Fig. 1.2. There are also other MSAs on compact optical transceivers, such as QSFP and consortiums on small-footprint, onboard optical I/O modules.

Among the platforms for photonic integration, silicon photonics provides most versatile platforms as ecosystems for design and fabrication of small-footprint photonic integrated circuits because it provides the precision, reliability, and mass-production capability established for complementary metal–oxide–semiconductor (CMOS) transistors.^{9–16} Active device elements, such as optical modulators and photodetectors, are integrated with passive device elements, such as optical couplers, filters, and multiplexers (including polarization diversity), using high-index-contrast optical waveguides in small footprints. Therefore, small-footprint, integrated, silicon-based optical modulators are extensively interested as keystones in optical signal transmission in high-capacity optical networks. Photonics ecosystems referred to in the next chapter allow design and fabrication of the integrated devices.

Energy efficiency is another critical subject in high-capacity optical networks to assure the sustainable growth of our communities, because high-capacity optical networks consume a considerable portion of the electrical energy supplied to all the infrastructures on the globe.^{17–22} More than 50% of the total electrical energy in the networks is spent on optical transceivers and related modules.^{19,22} Optical modulators require a significant portion of electrical energy input to the optical transceivers. Therefore, a reduction in electrical energy associated with optical modulators is a popular subject for energy efficiency in high-capacity optical networks, including reducing electrical energy for optical modulation and using thermo-electric cooling with optical modulators to maintain performance during modulation. A silicon-photonics platform based on high-index-contrast optical waveguides with a small footprint and refractive-index modulation in a broad spectral band with an extended temperature range provides feasible technical solutions for efficient optical modulators because it does not require a thermo-electric controller.

This book deals with integrated optical modulators as the key optical components for applications in optical-network domains at 100 Gb/s and beyond with a focus on silicon-photonics platforms. The integrated photonics platform has been developed from a CMOS-based design and microfabrication technologies, and versatile design and fabrication tools are available from

silicon-photonics foundries worldwide. A variety of device libraries that include electronic circuits have been supplied by such foundries. Therefore, readers can easily design, fabricate, and characterize integrated silicon-based optical modulators as key components in optical-network domains at 100 Gb/s and beyond.

Chapter 2 provides background details for integrated silicon-based optical modulators. It opens with a general overview of high-capacity optical networks. High-capacity optical networks at 100 Gb/s and beyond consist of several domains, which are constructed with fiber-optic links. The fiber-optic links are classified into two categories: a wavelength-division multiplexing (WDM) fiber link in the core, and metropolitan-area optical networks and parallel fiber-optic links in datacom applications, such as rack-to-rack optical interconnects in datacenters. The second half of the chapter presents the general aspects and principles of optical modulators in high-capacity optical networks. Semiconductor optical modulators are generally described as small-footprint optical modulators with an emphasis on integrated optical modulators in silicon-photonics platforms as photonic integrated circuits for optical signal generation in the most advanced compact-form-factor optical transceivers.

Generic integrated optical modulators are described in Chapter 3, classified in terms of electronic transition processes for optical modulation, schemes of optical modulation, and types of waveguide geometry. Among these, Mach–Zehnder (MZ) optical modulators using the free-carrier intraband electro-refraction effect are featured because of their superior broadband spectral response and the quality of optical intensity and phase modulation for optical modulators in high-capacity optical networks. Photonic integration in small-footprint optical modulators with a silicon-photonics platform for advanced modulation formats is described.

Chapter 4 covers optical circuits and waveguides in integrated MZ optical modulators. Optical layouts of the integrated MZ optical modulators suiting optical-signal generation in various modulation formats are described to clarify how the optical signals in the respective modulation formats are generated in the respective optical layouts. Simple mathematical models in the transfer-matrix framework are then presented with respect to some cases of the optical layouts to illustrate that fundamental mathematical methods such as matrix algebra are essential to the design and modeling of generic integrated MZ optical modulators. Integrated MZ optical modulators designed and fabricated on various material platforms consist of optical waveguides as the most fundamental building blocks. In particular, high index contrast in optical waveguides on silicon-photonics platforms allows for a very small core cross-section sub-micrometers wide and tall to construct a variety of small-footprint integrated photonic circuits. Optical waveguides and optical modes specifically on silicon-photonics platforms are also addressed.

Chapter 5 deals with electronic and opto-electronic properties of high-speed phase shifters as the most essential building blocks in integrated MZ optical modulators on compound-semiconductor and silicon-photonics platforms. In describing the physics of optical phase modulation, the Pockels effect typically used for modulators based on lithium-niobate electro-optic crystals is also included for comparison with intraband free-carrier plasma refraction and interband optical dipole transition processes, such as the Franz–Keldysh (FK) effect and optical Stark effect (QCSE) in group-IV semiconductors and III-V compound semiconductors under an electric field. Based on spectral and temperature dependences and frequency chirping of the carrier-induced optical phase-shifting processes, free-carrier plasma dispersion is shown to have the advantage of optical phase shifting over a broad spectral band within a wide range of temperature in semiconductor crystals that have inversion symmetry, which makes them useful for energy-efficient, small-footprint MZ optical modulators operating without thermo-electric cooling (TEC) for WDM optical transmission in high-capacity optical networks. Phase shifters based on free-carrier plasma dispersion consist of optical waveguides that contain PN junctions. The carrier concentration in a PN junction in a phase shifter is modulated under a high-frequency electric field; thus, high-speed optical phase modulation is realized via free-carrier plasma dispersion. Phase shifters based on free-carrier plasma dispersion are classified with respect to the profile of the PN junction (lateral or vertical PN junction). The chapter presents the technical procedure and characterization in simulation-based design and modeling of the PN-junction phase shifters to illustrate how to optimize the phase shifter performance.

Optical, electrical, and electro-optical characteristics of integrated silicon-based optical modulators are described in Chapter 6. Current–voltage characteristics and nanometer-scale images produced by scanning capacitance microscopy are presented as DC electrical characteristics. The microscopic capacitance images of the silicon-waveguide phase shifters are shown to be useful for visualizing the profiles of PN junctions in the phase shifters. Optical loss and optical phase shift are dealt with as DC optical characteristics. The integrated silicon-based optical modulators at 100 Gb/s and beyond are high-speed optical modulators with high-frequency radio-frequency (RF) metal electrodes. RF electrical and electro-optical characterizations based on S-parameter measurements provide high-frequency responses of traveling-wave electrodes and the integrated silicon-based optical modulators driven with RF signals fed to the phase shifters through the high-speed electrodes, as described in this chapter. A simple equivalent circuit model consisting of fundamental electrical circuit elements consisting of capacitors, inductors, and resistors is presented to analyze the high-speed characteristics of the modulators. The analysis of transients in optical modulation demonstrates that a simple equivalent circuit model consisting only of a capacitor and a

couple of resistors is sufficient for semi-quantitative analysis of high-speed phase shifters and allows for performance enhancement in high-speed optical modulation. Experimental evidence of temperature-insensitive optical modulation in the integrated silicon-based MZ optical modulators without TEC is also presented.

Optical-network domains, in which the integrated silicon-based MZ optical modulators are deployed, are classified in Chapter 7. The characteristics of the integrated silicon-based MZ optical modulators in transmission through optical-fiber links are then presented for various modulation formats in intensity modulation and phase modulation implemented in the optical-network domains. Subjects specific to the silicon-based optical modulators for the optical-network applications are noted. Subjects specific to the silicon-based optical modulators in the light of transmission characteristics are briefly summarized.

Photonic-electronic integration with silicon-based optical modulators is discussed with respect to two aspects in Chapter 8. Approaches of integration with electronic and photonic devices are discussed in the first part. The integration technologies are classified according to integration methods of devices from monolithic to package levels. Optical waveguides for vertical coupling are also discussed in terms of 3D photonic integration. Performance monitoring using photonic integrated circuits is an emerging subject; the chapter presents a photonic, integrated performance-monitoring circuit monolithically integrated with a silicon-based MZ optical modulator in a small-footprint chip on a silicon-photonics platform.

Supplemental technical items are compiled in an appendix to help readers better understand the contents of this book. These items include the bit rates and modulation formats adopted for optical signal transmission in high-capacity optical networks (Section A.1) and Kramers–Kronig transformation as a basic method for the characterization of the refractive index, and thus optical phase shift (Section A.2).

References

1. “Cisco visual networking index: forecast and methodology, 2015–2020,” <http://www.cisco.com/c/en/us/solutions/collateral/service-provider/visual-networking-index-vni/complete-white-paper-c11-481360.html>.
2. W. W. Rigrod and I. P. Kaminow, “Wide-band microwave light modulation,” *Proc. IEEE* **51**(1), 137–140 (1963).
3. C. J. Peters, “Gigacycle-bandwidth coherent-light traveling-wave amplitude modulator,” *Proc. IEEE* **53**(5), 455–460 (1965).
4. I. P. Kaminow and E. H. Turner, “Electrooptic light modulators,” *Proc. IEEE* **54**(10), 1374–1390 (1966).

5. S. Uehara, "Focusing-type optical modulator," *IEEE J. Quantum Electron.* **QE-9**(10), 984–986 (1977).
6. S. E. Miller, "Integrated optics: an introduction," *Bell System Tech. J.* **48**(7), 2059–2069 (1969).
7. P. K. Tien, "Light waves in thin films and integrated optics," *Appl. Opt.* **10**(11) 2395–2413 (1971).
8. "Next gen PMD CFP MSA baseline specifications," http://www.cfp-msa.org/Documents/CFP_MSA_baseline_specifications_15.pdf.
9. G. T. Reed and A. P. Knights, *Silicon Photonics: An Introduction*, John Wiley and Sons, Chichester, UK (2004).
10. M. Hochberg, "Towards fabless silicon photonics," *Nature Photon.* **4**(8), 492–494 (2010).
11. T. Pinguet, S. Gloeckner, G. Masini, and A. Mekis, "CMOS photonics: a platform for optoelectronics integration," in *Silicon Photonics II: Components and Integration*, D. J. Lockwood and L. Pavesi, Eds, Topics in Applied Physics **119**, Springer-Verlag, Berlin Heidelberg, 187–216 (2011).
12. T. Baehr-Jones, T. Pinguet, G.-Q. Lo, S. Danziger, D. Prather, and M. Hochberg, "Myths and rumours of silicon photonics," *Nature Photon.* **6**(4), 206–208 (2012).
13. M. A. Popović, et al., "Monolithic silicon photonics in a sub-100nm SOI CMOS microprocessor foundry: progress from devices to systems," *Proc. SPIE* **9367**, 93670M-1–93670M-10 (2015).
14. M. Heins, et al., "Design flow automation for silicon photonics: challenges, collaboration, and standardization," in *Silicon Photonics III: Systems and Applications*, D. J. Lockwood and L. Pavesi, Eds, Topics in Applied Physics **122**, Springer-Verlag, Berlin Heidelberg, 99–156 (2016).
15. A. E.-J. Lim, et al., "Path to silicon photonics commercialization: the foundry model discussion," in *Silicon Photonics III: Systems and Applications*, D. J. Lockwood and L. Pavesi, Eds, Topics in Applied Physics **122**, Springer-Verlag, Berlin Heidelberg, 191–216 (2016).
16. T. L. Koch, et al., "The American Institute for Manufacturing Integrated Photonics: advancing the ecosystem," *Proc. SPIE* **9772**, 977202-1–977202-6 (2016).
17. Y. Zhang, P. Chowdhury, M. Tornatore, and B. Mukherjee, "Energy efficiency in telecom optical networks," *IEEE Commun. Survey & Tutorials* **12**(4), 441–458 (2010).
18. O. Tamm, C. Hermsmeyer, and A. M. Rush, "Eco-sustainable system and network architectures for future transport networks," *Bell Labs Tech. J.* **12**(4), 311–328 (2010).
19. K. Ishii, J. Kurumida, S. Namiki, T. Hasama, and H. Ishikawa, "Energy consumption and traffic scaling of dynamic optical path networks," *Proc. SPIE* **8646**, 86460A-1–86460A-10 (2013).

-
20. P.-H. Ho, G. Shen, S. Subramaniam, H. T. Mouftah, C. Qiao, and L. Wosinska, “Guest editorial energy-efficiency in optical networks,” *IEEE J. Sel. Areas Commun.* **32**(8), 1521–1523 (2014).
 21. Y. Demir and N. Hardavellas, “Towards energy-efficient photonic interconnects,” *Proc. SPIE* **9368**, 93680T-1–93680T-12 (2015).
 22. H. Isono, “Recent standardization directions on high-speed client and line side components,” *Proc. SPIE* **9775**, 97750C-1–97750C-8 (2016).